11TH INTERNATIONAL SCIENTIFIC CONFERENCE ON DEFENSIVE TECHNOLOGIES
OTEH 2024
Serbia, Tara, 9-11 October 2024

MAGNETOIMPEDANCE EFFECT OF NANOCRYSTALLINE FeNiSiB and FeCuVSiB RIBBONS

RADOSLAV SURLA
Military Technical Institute, Belgrade, Serbia, ekorade@gmail.com

MILICA M. VASIĆ
Faculty of Physical Chemistry, University of Belgrade, Belgrade, Serbia, mvasic@ffh.bg.ac.rs

DRAGICA M. MINIĆ
Faculty of Physical Chemistry, University of Belgrade, Belgrade, Serbia, dminic@ffh.bg.ac.rs

LJUBICA RADOVIĆ
Military Technical Institute, Belgrade, Serbia, ljubica.radovic@mod.gov.rs

NEBOJŠA MITROVIĆ,
Faculty of Technical Sciences, University of Kragujevac, Serbia, nebojsa.mitrovic@ftn.kg.ac.rs

PAVEL CRNOMARKOVIĆ,
Military Technical Institute, Belgrade, Serbia, pavel@ptt.rs

Abstract: *The Magnetoimpedance (MI) effect of Fe-based nanostructured alloy ribbons $Fe_{72}Ni_8Si_{10}B_{10}$ (A) and $Fe_{72}Cu_1V_4Si_{15}B_8$ (B) was studied, compared for the two ribbons, and finally correlated with their composition and microstructure. The nanostructured ribbons were prepared by melt-spinning on a cold rotating disk. Basic characterization of the studied ribbons was performed by XRD and SEM-EDX techniques. It was found that the MI ratio of ribbon A is significantly lower than that of ribbon B, but the effects were observed at different frequencies. The maximal MI ratio of ribbon A was detected at 57.57 MHz, while in the case of ribbon B, that was the frequency of about 13 MHz. The structure of both ribbons consists of a certain amount of nanocrystals, α-(Fe, Ni) for the ribbon A and α-Fe(Si) for the ribbon B, which are embedded in an amorphous matrix. The MI effect and the frequency of its maximum are determined by the mobility of the magnetic domains in the samples, which is correlated with the microstructural specificities of individual ribbons.*

Keywords: *Magnetoimpedance effect, nanostructure, melt-spinning, α-Fe(Si), α-(Fe, Ni)*

1. INTRODUCTION

Magnetoimpedance (MI) effect is defined as the influence of external DC field on the change in impedance of ferromagnetic sample. It was discovered at the beginning of the last decade of the twentieth century, and nowadays, it is applied in magnetic field sensors with high sensitivity [1-5]. Some ferromagnetic amorphous / nanocrystalline alloys were found to exhibit the MI effect.

The impedance of ferromagnetic material declines with an increase in magnetic field, but on the other hand, it grows with an increase in the frequency of the current flowing through the sample.

Most commonly, the MI ratio is expressed using the following equation:

$$\Delta Z/Z(\%)=100\% \cdot(Z(H)-Z(H_{max}))/Z(H_{max}), \quad (1)$$

where $Z(H_{max})$ is impedance at the maximum value of external magnetic field. Depending on the material considered, at H=0, the remanent magnetization can affect the impedance, and further, with increase in magnetic field, such magnetization become annulled, resulting in asymmetry of MI-diagram for different magnetic field directions (–H and +H).

The dependence of magnetoimpedance on frequency is related to the skin effect. This effect is characterized by penetration depth, which grows with an increase in magnetic field (due to decrease in magnetic permeability), and decline with increase in frequency. Alternating current causes the occurrence of eddy currents, which include the grouping of charges that transmit the electrical energy to the peripheral parts of the conductor. The skin depth can be defined as:

$$\delta_m=(\rho/(\pi\cdot\mu\cdot f))^{-1}, \quad (2)$$

where ρ is specific electrical resistivity, μ is magnetic permeability, and f is frequency.

Beside the aforementioned, the MI ratio depends on the

Corresponding author: R. Surla;
E-mail: ekorade@gmail.com
DOI: 10.5937/OTEH24098S

domain structure of magnetic material, which is determined by the material composition and microstructure, and is closely related to the preparation technology.

The maximal MI ratio occurs at specific values of external magnetic field and frequency of the current flowing through the sample. It can be determined experimentally, and it is tightly related to the microstructure of the material.

2. EXPERIMENTAL PROCEDURE

In this work, the $Fe_{72}Ni_8Si_{10}B_{10}$ ribbon-shaped alloy (A) was subjected to experimental measurements of magnetoimpedance, and then compared with our previous MI research [4, 6] of the $Fe_{72}Cu_1V_4Si_{15}B_8$ ribbon (B). The ribbon-shaped alloys, 1.5 mm wide, were prepared by melt-quenching, which included rapid cooling of the melt on a cold wheel rotating at 2000 rpm. The average thickness of the alloys A and B is around 55 μm [7].

Microstructure of the studied alloys was examined by means of X-ray diffraction analysis (XRD). For this purpose, a Rigaku SmartLab diffractometer equipped with a Cu Kα radiation source was used. Rietveld refinement was conducted to estimate the contents and microstructural parameters of individual phases in the samples. Scanning electron microscopy (SEM), with a SEM JEOL JSM-6610-LV microscope, was carried out to examine the surface morphology of the samples (shiny side).

In order to study the magnetoimpedance effect of the ribbons, measurements of the impedance were performed in homogeneous magnetic field of 15 kA/m, generated using the pair of Helmholtz coils, with an instrument Vector Network Analyser Agilent 8753ES. The sample holder was specially designed to allow measurements on the ribbon-shaped samples, 1 cm in length.

3. RESULTS AND DISCUSSION

3.1 XRD analysis

XRD analysis of the as-cast alloy ribbons reveals the composite structure, including the presence of crystalline phases in the samples, beside the amorphous matrix, Figures 1 and 2.

The abundance of crystalline grains inside the ribbon is not homogeneous due to differences in cooling rates occurring during the ribbon preparation. Namely, the wheel-side of the ribbon (matte side) is cooled faster and thus solidificates faster than the opposite (shiny) side, resulting in larger crystalline fraction at the shiny side of the ribbon, Table 1.

Figures 1 and 2 represents the XRD patterns of the A and B alloy ribbons, respectively, indicating the alloy structure consisted of bcc iron (α) crystals embedded in amorphous matrix. The bcc iron phase is denoted as α-(Fe, Ni) and α-Fe(Si) in the case of A and B, respectively, Figures 1 and 2, considering the solubility of Si and Ni elements in the bcc iron structure.

The average crystallite size of the bcc iron phase was estimated from the XRD patterns for both ribbons, amounting to 53 and 40 nm for A and B, respectively.

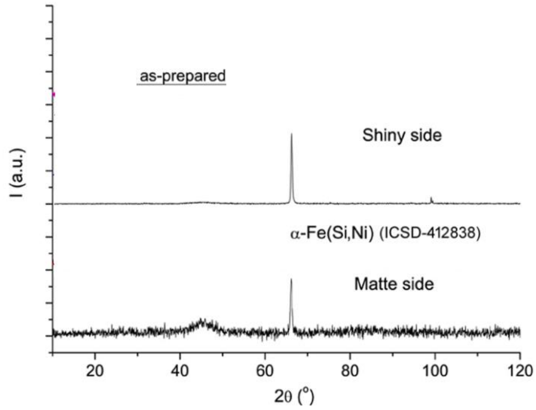

Figure 1. XRD patterns of the $Fe_{72}Ni_8Si_{10}B_{10}$ (A) alloy ribbon.

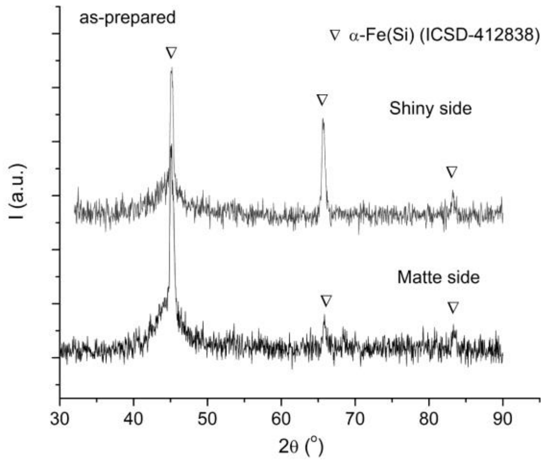

Figure 2. XRD patterns of the $Fe_{72}Cu_1V_4Si_{15}B_8$ (B) alloy ribbon.

Table 1. Weight fraction of the bcc iron crystalline structure at matte and shiny sides of the studied ribbons.

Ribbon	Matte side	Shiny side
$Fe_{72}Ni_8Si_{10}B_{10}$ (A)	5 wt.%	14 wt.%
$Fe_{72}Cu_1V_4Si_{15}B_8$ (B)	18 wt.%	20 wt.%

3.2 SEM analysis

Relatively uniform surface morphology of both ribbons, A and B, can be observed in the SEM micrographs presented in Figures 3 and 4. Some dents at the surface of the ribbons resulted from the preparation procedure, including melt quenching.

EDX analysis, performed in the regions marked on the micrographs, confirmed the presence of the elements specified in the alloy designation, at the ribbon surface, Table 2.

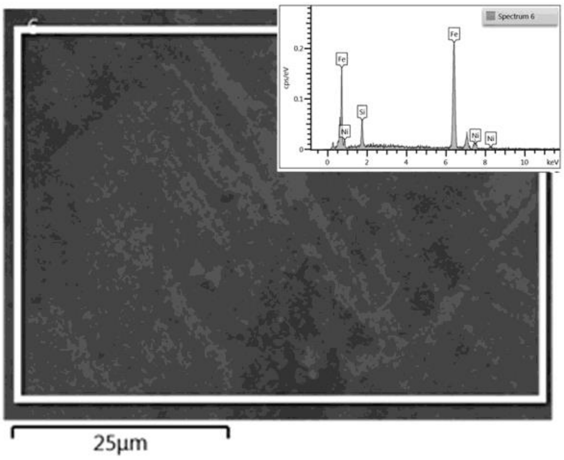

Figure 3. SEM micrograph (with EDX spectrum) of the as-cast $Fe_{72}Ni_8Si_{10}B_{10}$ (A) alloy ribbon.

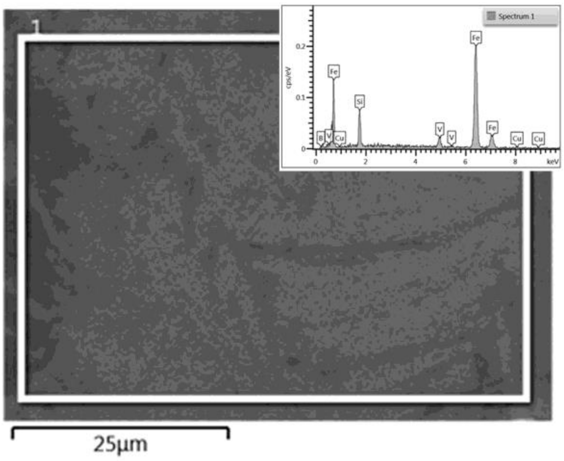

Figure 4. SEM micrograph (with EDX spectrum) of the as-cast $Fe_{72}Cu_1V_4Si_{15}B_8$ (B) alloy ribbon.

Table 2. Results of the EDX analyses (at. %) performed for the alloy ribbons studied in the work.

	Fe	Ni	Si	
$Fe_{72}Ni_8Si_{10}B_{10}$	79.3	9.6	11.1	
	Fe	Cu	V	Si
$Fe_{72}Cu_1V_4Si_{15}B_8$	79.1	1.1	4.5	15.3

3.3. Magnetoimpedance measurements

The MI ratio of the $Fe_{72}Ni_8Si_{10}B_{10}$ (A) alloy ribbon at various frequencies and magnetic fields was studied, and the obtained results are presented in Figures 5-8. The maximal MI ratio, 26%, is observed for frequencies 57-58 MHz (MI_{max}= 26% for f= 57.57 MHz and H= 847.2 A/m, while H_{max}=15kA/m).The dependence of MI ratio of A on frequency for various magnetic field values is presented in Figures 5 and 6. The effect grows with increase in magnetic field up to 847.2A/m (Figure 5), while further increase in magnetic field leads to decline in the MI ratio (Figure 6).

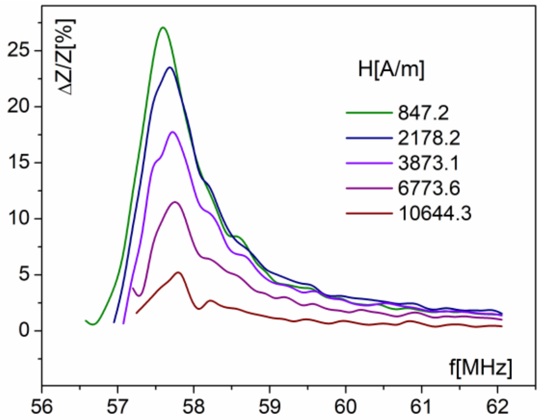

Figure 5. Dependence of MI ratio of $Fe_{72}Ni_8Si_{10}B_{10}$ (A) alloy ribbon on frequency for magnetic field ranging 0-847.2 A/m; H_{max}=15 kA/m.

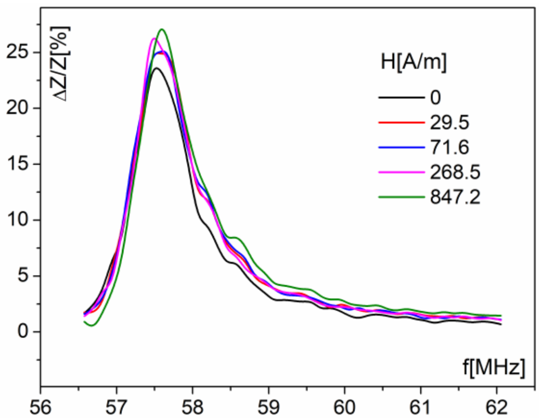

Figure 6. Dependence of MI ratio of $Fe_{72}Ni_8Si_{10}B_{10}$ (A) alloy ribbon on frequency for magnetic field ranging 847.2-10644 A/m; H_{max}=15 kA/m.

Figures 7 and 8 show the dependence of MI ratio of A on magnetic field for characteristic frequencies. The growth of the MI ratio with frequency up to f= 57.57 MHz, Figure 7, and decline of the MI ratio with further increase in frequency (f > 57.57 Hz, Figure 8) can be observed.

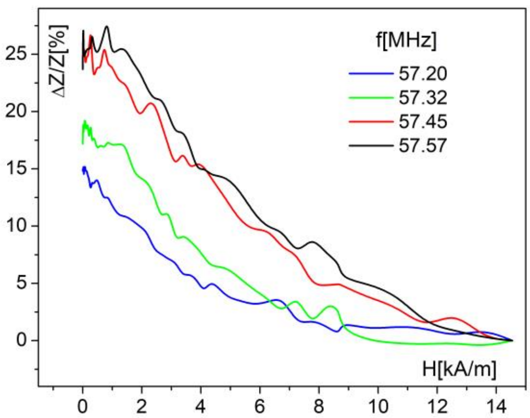

Figure 7. Dependence of MI ratio of $Fe_{72}Ni_8Si_{10}B_{10}$ (A) alloy ribbon on magnetic field for frequency ranging 57.2-57.57 MHz; H_{max}=15 kA/m.

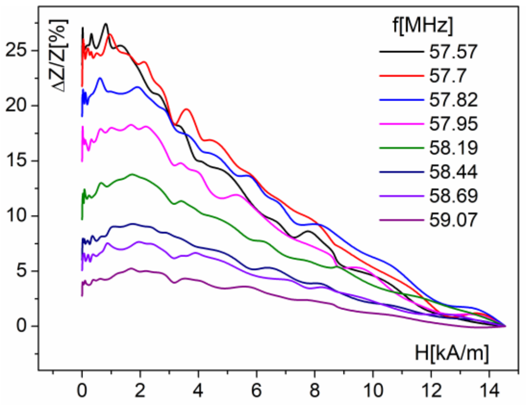

Figure 8. Dependence of MI ratio of $Fe_{72}Ni_8Si_{10}B_{10}$ (A) alloy ribbon on magnetic field for frequency ranging 57.57-59.07 MHz; H_{max}=15 kA/m.

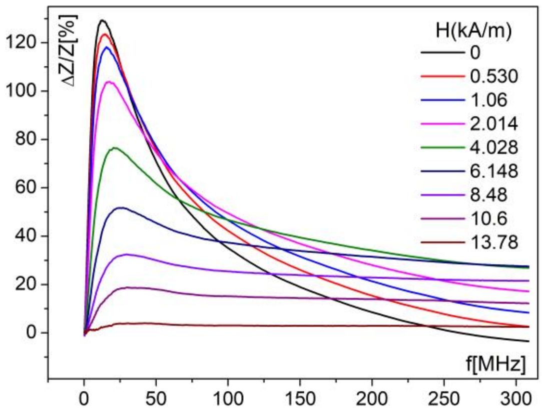

Figure 9. Dependence of MI ratio of $Fe_{72}Cu_1V_4Si_{15}B_8$ (B) alloy ribbon on frequency for positive magnetic field ranging 0-13.8 kA/m; H_{max}=14.8 kA/m.

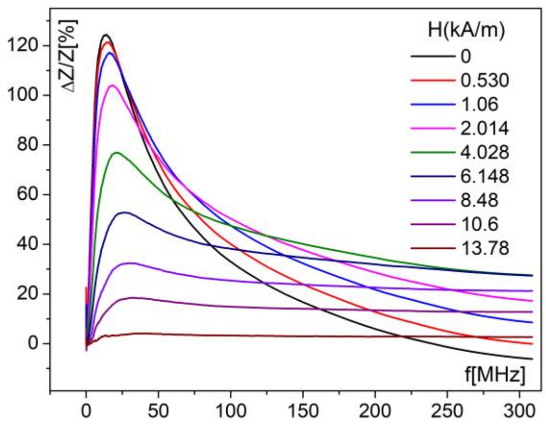

Figure 10. Dependence of MI ratio of $Fe_{72}Cu_1V_4Si_{15}B_8$ (B) alloy ribbon on frequency for negative magnetic field ranging 0-13.8 kA/m; H_{max}=14.8 kA/m.

The maximal MI ratio of the $Fe_{72}Cu_1V_4Si_{15}B_8$ (B) alloy ribbon, obtained for H_{max} of around 15 kA/m, amounts to 125-129% (129% for f= 13 MHz, H= 0 and + direction, and 125% for f= 12.5 MHz, H= 106 A/m and - direction), Figures 9-12, and it is several times larger than that of the ribbon A. By the way, our previous research of the ribbon B [4] revealed MI_{max}= 153%, but for H_{max}=21.2 kA/m (f= 18.55 MHz and H= 0 A/m).

Better MI ratio of the ribbon B than that of the ribbon A can be attributed to better mobility of magnetic domains in the case of B, which is related to the microstructure and composition of the material. Crystal size is very important microstructural parameter, where it is thought that the nanocrystal size lower than the magnetic exchange length considerably reduces the contribution of magnetocrystalline anisotropy of the nanocrystals to the overall magnetic anisotropy of the material [8, 9], affecting its overall magnetic behavior. For Fe-based alloys, the ferromagnetic exchange length is 20-40 nm [10]. For the studied alloy ribbons, A and B, certain difference in the crystallite size of the bcc iron phase is observed (53 nm for A, and 40 nm for B), which has an effect on the average anisotropy, considering its proportionality to the sixth power of the crystal size [10]. For the crystals formed in the as-cast ribbons, the crystallite size is connected with the chemical composition of the alloy. In the B ribbon, Cu and V elements are present, where Cu makes the nucleation process faster and V decreases the crystal growth rate, thus yielding lower crystallite size than that of the Fe-based alloys without such additives, while similar components are not present in the ribbon A.

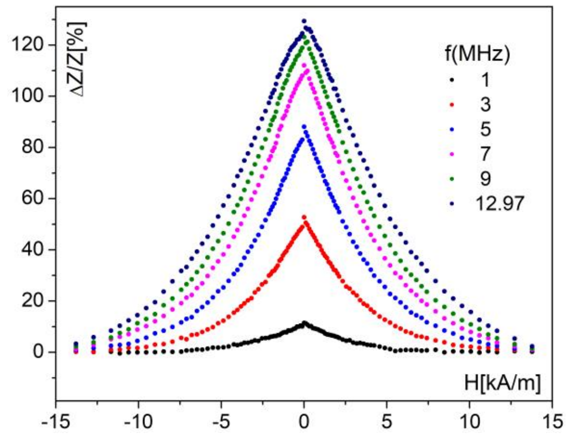

Figure 11. Dependence of MI ratio of $Fe_{72}Cu_1V_4Si_{15}B_8$ (B) alloy ribbon on magnetic field for frequency ranging 1-13 MHz; H_{max}= ±14.8 kA/m.

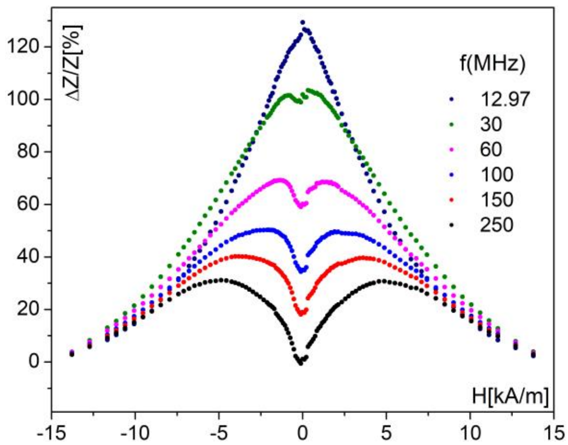

Figure 12. Dependence of MI ratio of $Fe_{72}Cu_1V_4Si_{15}B_8$ (B) alloy ribbon on magnetic field for frequency ranging 13-250 MHz; Hmax= ±14.8 kA/m.

5. CONCLUSION

The magnetoimpedance effect is observed for both alloys studied in this work, suggesting their potential application in MI sensors. The effect is more pronounced for the $Fe_{72}Cu_1V_4Si_{15}B_8$ (B) alloy, and thus its magnetoimpedance sensitivity to an external magnetic field is larger. The MI effect of the $Fe_{72}Ni_8Si_{10}B_{10}$ (A) is weaker and occurs at higher frequencies. The MI effect is significantly dependent on the microstructure of the materials. The microstructure consisted of the bcc iron (α) crystals embedded in amorphous matrix is crucial for the magnetic behavior of both alloys. Appropriate choice of chemical composition of the material and preparation conditions allow the production of alloy ribbons with desired microstructure, and thus the design of materials with targeted properties, in this case potentially applicable in the MI elements.

Acknowledgments

This work was supported in part by the Ministry of Science, Technological Development and Innovation of the Republic of Serbia, Faculty of Technical Sciences Čačak, University of Kragujevac under Grant 451-03-66/2024-03/200132, Faculty of Physical Chemistry, University of Belgrade, under Grant 451-03-66/2024-03/200146, and Military Technical Insitute under grant 451-03-66/2024-03/200325.

References

[1] Panina, L.V., Mohri, K.: *Magneto-impedance Effect in Amorphous Wires*, Applied Physics Letters, 65(9), (1994), 1189 – 1191.

[2] Kraus, L.: *Theory of Giant Magneto-impedance in the Planar Conductor with Uniaxial Magnetic Anisotropy*, Journal of Magnetism and Magnetic Materials, 195(3), (1999), 764 – 778.

[3] Surla, R., Mitrović, N., Đukić, S., Ibrahimović, V.: *Amorphous* $Fe_{72}Cu_1V_4Si_{15}B_8$ *Ribbon as Magneto-Impedance Sensing Element*, Serbian Journal of Electrical Engineering, 13(3), (2016), 381-394.

[4] Surla, R., M., Vasić, Mitrović, N., Radović, Lj., Minić, D.: *Magnetic properties of* $Fe_{72}Cu_1V_4Si_{15}B_8$ *alloy with a composite amorphous/ nanocrystalline structure*, Journal of Magnetism and Magnetic Materials, 564 (2022) 170141

[5] SURLA, R.: Doktorska disertacija: *Uticaj odgrevanja na strukturne transformacije i magnetna svojstva legure* $Fe_{72}Cu_1V_4Si_{15}B_8$, FTN Čačak, Univerzitet u Kragujevcu, 2021.

[6] Vasić M., Surla R., Mitrović N., Minić Dragica., Mitrović N., Maričić A., Minić Dušan: *Thermally induced microstructural transformations of* $Fe_{72}Cu_1V_4Si_{15}B_8$ *alloy*, Metal. Mater. Trans. A 48 (2017) 4393–4402.

[7] Surla, R., M., Vasić, Mitrović, N., Minić, D.: *Synthesis and characterization of* $Fe_{72}Cu_1V_4Si_{15}B_8$ *metallic glass ribbons prepared by melt spinning casting*, 9^{th} International Scientific Conferenceon Defensive Technologies, Belgrade, 8-9, October 2020.

[8] Herzer, G.: *Grain structure and magnetism of nanocrystalline ferromagnets*, IEEE Transactions on Magnetics, 25 (1989) 3327-3329.

[9] Kulik, T.: *Nanocrystallization of metallic glasses*, Journal of Non-crystalline Solids, 287 (2001) 145-161.

[10] Herzer, G.: *Anisotropies in soft magnetic nanocrystalline alloys*, Journal of Magnetism and Magnetic Materials, 294 (2005) 99-106.